EXPERIMENTAL STUDY OF FPS SYSTEM IN BRIDGE SEISMIC ISOLATION

P. TSOPELAS AND M. C. CONSTANTINOU
Department of Civil Engineering, State University of New York, Buffalo, NY 14260, U.S.A.

Y. S. KIM
Institute of Construction Technology, Kumho Construction Co., Seoul, Korea

AND

S. OKAMOTO
Technology Research Center, Taisei Corporation, Yokohama, Japan, 245

SUMMARY

An experimental study of a seismically isolated and a comparable non-isolated bridge is presented. The bridge model featured flexible piers, weighed 158 kN and was tested on a shake table with an array of real and simulated seismic motions with peak acceleration in the range 0·1–1·1g. When isolated, the bridge deck was supported by four spherically shaped sliding bearings (known as Friction Pendulum System or FPS bearings) with friction coefficient under dynamic conditions in the range 0·07–0·12. The experimental results demonstrated a substantial improvement in the ability of the isolated bridge to sustain all levels of seismic excitation under elastic conditions.

KEY WORDS: seismic isolation; bridges; earthquakes; testing; sliding bearings; shaking table

INTRODUCTION

Contemporary techniques of seismic hazard mitigation in bridges include seismic isolation and energy dissipation. The seismic isolation strategy attempts to reduce the seismic inertia forces to or near the elastic capacity of a bridge, thus eliminating or reducing inelastic deformation and damage to the substructure. It may also be used for distributing the seismic forces to elements of the substructure in a predetermined pattern. Fundamental in the seismic isolation strategy is the lengthening of the period of the system. Seismic isolation systems with strong restoring force have been used in bridges in New Zealand and the United States.[1,2] Over 75 isolated bridges in the United States are currently completed or under construction.

Italian engineers constructed over 150 bridges[3] using isolation systems with nearly elastoplastic behaviour. A large number of these bridges is isolated only in the longitudinal direction (referred to as partial or unidirectional isolation). Typically, these systems consist of lubricated sliding bearings with yielding mild steel dampers. Such systems offer the advantage of constant force transmitted to the substructure, independent of the seismic action. However, they are characterized by the development of permanent displacement and by a large dispersion in peak displacement response.[4]

Japan followed a different approach at protecting bridges. The bridge design spectra in Japan contain, depending on the soil conditions, constant spectral accelerations of periods of 1·4 and 2 sec. For effective seismic isolation, it would be required to lengthen the period of the system to values beyond 3 sec, which is very difficult to achieve and results in undesirable large bearing displacements. Hence, Japanese engineers prefer the use of stiff isolation bearings in order to enhance energy dissipation and achieve effective distribution of lateral forces. This approach is called "Menshin".[5]

In 1991, the University at Buffalo and Taisei Corporation, Japan, began a research program on the study of seismic protective systems for bridges. While the project contained a major task for the development of

CCC 0098–8847/96/010065–14

Received 7 February 1995
Revised 24 July 1995

a bridge seismic isolation system for application in Japan,[6] it also had as an objective to study established isolation systems which were not previously tested within a bridge model. These included the Italian elastoplastic systems[4] and the spherical sliding FPS system.[7] This paper describes the results obtained in the testing of the latter system.

PRINCIPLES OF OPERATION AND MODELLING OF FPS BEARINGS

Zayas *et al.*[8] described the FPS bearing and its principles of operation and presented experimental results of its behaviour from testing of a small building model. Since then, Mokha *et al.*[9] and Al-Hussaini *et al.*[10] presented experimental studies of isolated large moment resisting and braced frames with FPS bearings.

The FPS bearing is a form of sliding bearing consisting of an articulated slider on a spherical surface. Figure 1 shows a free body diagram of an FPS bearing from where it may be readily derived that the lateral force F needed to produce a displacement u is given by

$$F = \frac{W}{R\cos\theta}u + \frac{F_f}{\cos\theta} \tag{1}$$

where W is the load carried by the bearing, R is the radius of curvature of the spherical surface, F_f is the friction force and θ is the angle of rotation. Since the bearings are typically designed to have a displacement capacity $u < 0{\cdot}2R$, it follows that $1/\cos\theta < 1{\cdot}02$ and without significant error, equation (1) may be linearized to the form

$$F = \frac{W^*}{R}u + \mu W^* Z \tag{2}$$

in which now W^* stands for the instantaneous axial load (includes the gravity load plus the effects of vertical ground motion and overturning moment), μ is the velocity and pressure-dependent coefficient of friction and

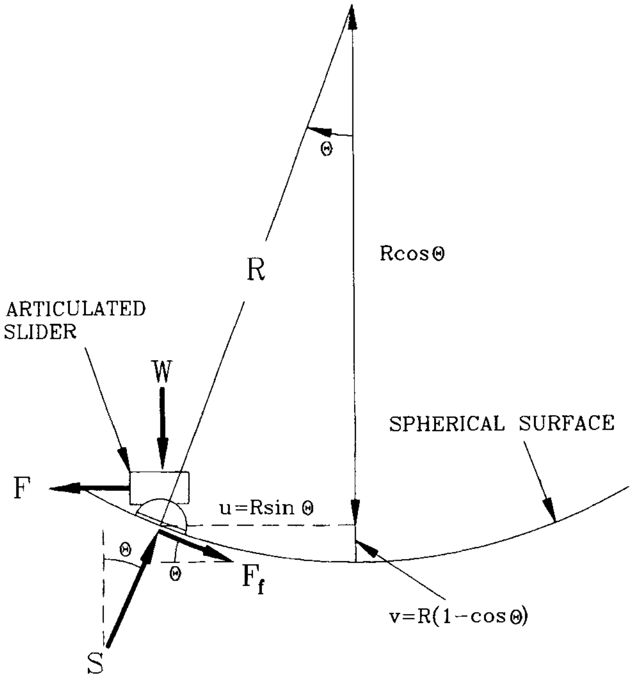

Figure 1. Free body diagram of FPS bearing

Z is a variable in the range $(-1, 1)$,[7] which depends on the direction of the instantaneous velocity vector.

In general, the coefficient of friction may be described[2,7] by

$$\mu = f_{max} - (f_{max} - f_{min}) \exp(-a|\dot{u}|) \tag{3}$$

$$f_{max} = f_{max\,o} - \Delta f \tanh(\alpha p) \tag{4}$$

where f_{min} is the coefficient of friction at essentially zero velocity of sliding, f_{max} is the coefficient of friction at large velocity of sliding, $\dot{u}$ is the instantaneous velocity of sliding, p is the instantaneous pressure, and a, α, $f_{max\,o}$ and Δf are parameters. It should be noted that in this model only the value of friction coefficient at large velocity of sliding (f_{max}) is assumed to be dependent on the bearing pressure. This model represents an approximation of a more complex behaviour.[2]

Equation (2) reveals a fundamental property of the FPS bearing. The lateral force is directly proportional to the axial load; a property which minimizes unfavourable torsional motions. The same property results also in an unfavourable fluctuation of the lateral bearing force under conditions of strong vertical acceleration.

BRIDGE MODEL AND TEST PROGRAM

Figure 2 shows the tested bridge model. It was designed to have flexible piers so that under non-isolated conditions the fundamental period of the model in the longitudinal direction was 0·25 sec (or 0·5 sec in prototype scale). At quarter length scale, it had a total weight of 157·8 kN (35·5 kips) with a deck weight of 140 kN (31·5 kips). The piers were detailed to yield under the combined effects of gravity load (40 kN each column) and 50 per cent of the gravity load applied as horizontal load at each bearing location. The fundamental period and the damping ratio of the bridge model with fixed bearings (fixed against translational movement but not rotation) were determined in identification tests with a 0–20 Hz banded white noise of 0·03g peak acceleration, and found to be 0·26 sec and 0·02 of critical, respectively. Additional identification tests of the model were conducted with white noise input of 0·1g peak table acceleration to obtain a fundamental period of 0·25 sec and corresponding damping ratio of 0·04 of critical. Estimates of damping ratio from loops of pier shear force versus pier deformation during shake table testing of the non-isolated

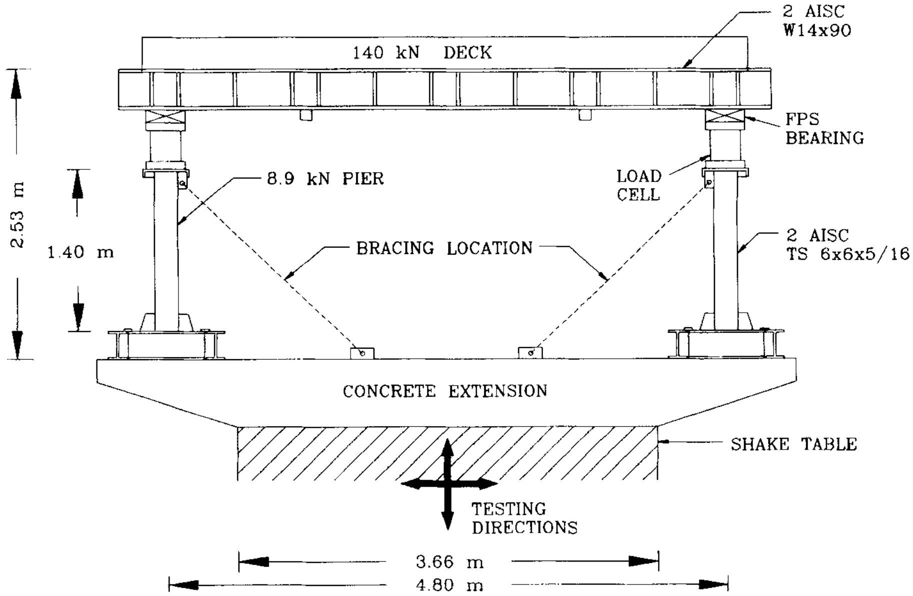

Figure 2. Quarter scale bridge model

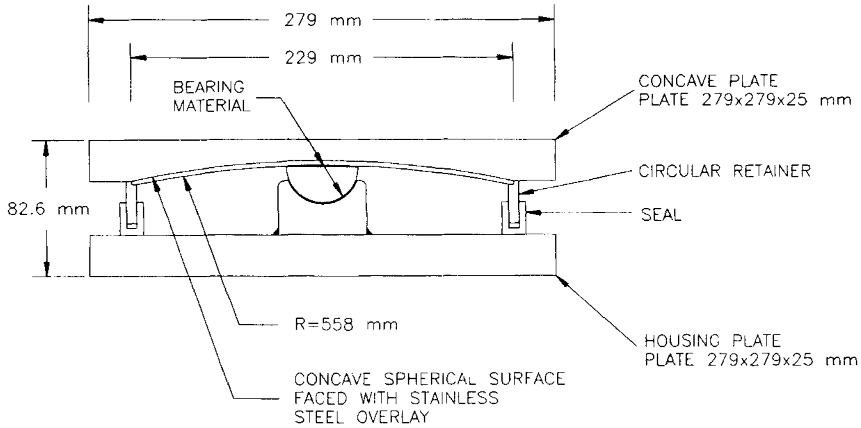

Figure 3. Construction of friction pendulum system bearing

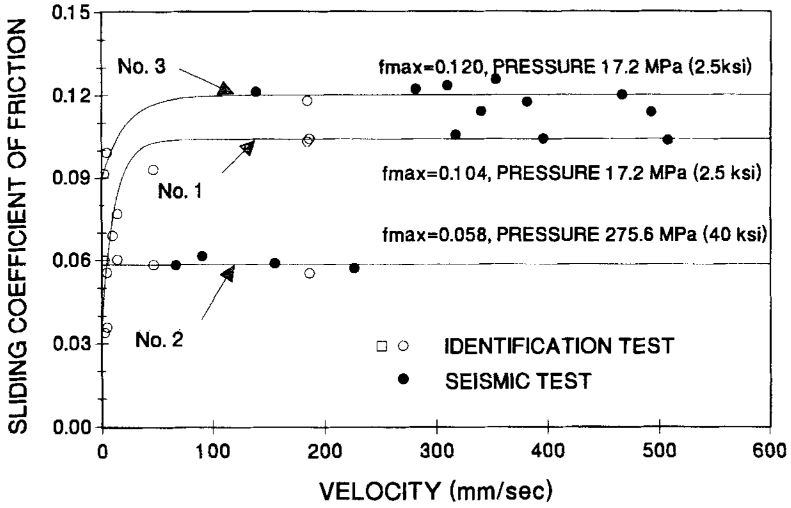

Figure 4. Coefficient of friction of bearings

model were in the range of 0·04 to 0·08 of critical. These loops displayed higher damping as a result of hysteretic action in the concrete extension of the shake table. Thus while the columns of the pier remained elastic, the pier system displayed realistic hysteretic action with equivalent damping ratio of at least 5 per cent of critical.

When isolated the deck was supported by four FPS bearings on top of the piers. Figure 3 shows the bearing construction. The bearings had a radius of curvature $R = 558{\cdot}8$ mm and displacement capacity of 89 mm. They were installed with the spherical surface facing down. For this radius of curvature the period of vibration of the isolated rigid deck is 1·5 sec (or 3 sec in prototype scale).

The fractional properties of the bearings were identified while the bridge model was on the shake table by conducting harmonic motion tests.[7] The measured coefficient of friction and the identified parameters of the bearings (equations (3) and (4)) are presented in Figure 4 and Table I. Three different composite materials were used in contact with polished stainless steel in the bearings. Of these, material No. 1 was the PTFE-based composite typically used in FPS bearings, whereas materials No. 2 and 3 were other high bearing capacity and low wear composites. Material No. 2 was used at high bearing pressure in order to achieve a low friction coefficient. It exhibited a friction coefficient value which was independent of velocity

Table I. Identified parameters in model of friction of bearings

Material	Bearing pressure (MPa)	f_{min}	f^*_{max}	a (s/m)	f_{maxo}	Δf	α (MPa^{-1})
No. 1	17·2	0·040	0·104	83·4	0·120	0·070	0·012
No. 2	275·6	0·058	0·058	†	N.A.	N.A.	N.A.
No. 3	17·2	0·090	0·120	47·0	N.A.	N.A.	N.A.

*Value at indicated bearing pressure
†Coulomb friction

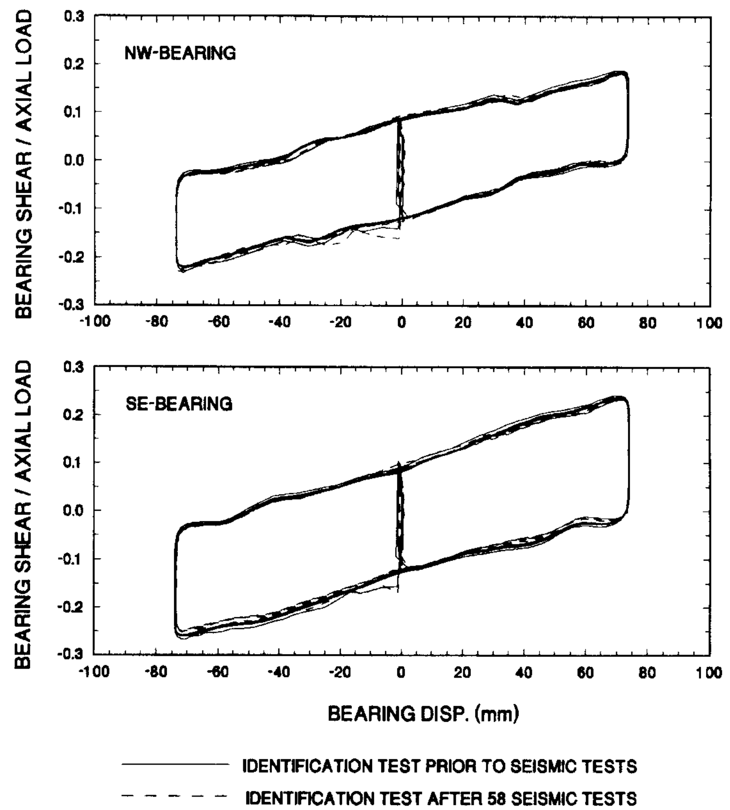

Figure 5. Recorded force-displacement loops of bearings with material No. 1

(Coulomb friction). Materials 1 and 3 were used at low bearing pressure so that they exhibited high velocity friction in the range of 0·10 to 0·12.

While materials No. 1 and 3 provided about the same characteristic strength to the isolation system, material No. 1 exhibited two significant advantages. First it had a very low value of friction coefficient at nearly zero sliding velocity. Thus while the two systems with materials No. 1 and 3 resulted in nearly identical peak bearing displacement and substructure response, the system with material No. 1 had significantly smaller permanent displacements than the other system. Second, it had stable properties over a large number of cycles in repeated testing. Figure 5 provides evidence of this desirable property. The figure shows loops of force versus displacement of two of the bearings as recorded in tests of five cycles of harmonic motion of 75 mm amplitude and frequency of 0·4 Hz (peak velocity = 188 mm/sec). The bearings were under load of

35 kN (pressure of 17·2 MPa). It can be observed that the loops do not change between the initial identification test and in an identical test following 58 high velocity seismic tests.

The bridge model was tested in the non-isolated (bearings locked by side plates) and in several isolated configurations. These included configurations with two flexible piers (model of a multiple span bridge), one flexible and one stiff (braced—see Figure 2) piers (model of a two-span bridge) and two stiff piers (model of single-span bridge).

A total of 173 seismic tests and a number of identification tests were conducted. Tests were conducted with only horizontal input and with combined horizontal and vertical input. However, due to the vertical flexibility of the overhangs of the shake table (Figure 2) the bridge model underwent significant vertical motion in all tests, even in those with only horizontal input. The earthquake signals are listed in Table II and consisted of historic earthquakes and artificial motions compatible with:

(a) The Japanese bridge design spectra for levels 1 and 2 and ground conditions 1 (rock), 2 (alluvium) and 3 (deep alluvium).[11]
(b) The California Department of Transportation (CalTrans) bridge spectra.[12] These motions were identical to those used in the testing of another bridge model by Constantinou *et al.*[13]

Each record was compressed in time by a factor of two to satisfy the similitude requirements.

EXPERIMENTAL RESULTS

The report of Constantinou *et al.*[7] contains a detailed presentation of the experimental results. Herein results are presented only condensed and primarily in the form of comparison between isolated and non-isolated configurations. The presented results include the bearing displacement and the pier shear force. The latter is the force at pier mid-height (as measured by strain-gage load cells), and is not the force transmitted by the bearings to the pier top. Typically, the pier shear force is larger than the bearing force at the top of the pier due to the contribution of pier top inertia forces. All results are presented in model scale unless otherwise stated.

The isolation system with low friction ($f_{max} = 0{\cdot}058$) and isolation period of 1·5 s (3 s in prototype scale) are appropriate for application in areas of low to moderate seismicity. Accordingly, tests were primarily conducted with moderate excitations. Peak ground acceleration in these seismic motions varied between $0{\cdot}13g$ and $0{\cdot}45g$. The test results are summarized in Table III, where they are compared to the results of the non-isolated bridge. The latter results were either directly obtained in tests or extrapolated from test results of the non-isolated bridge by assuming linear behaviour and provided that the extrapolated response did not exceed the theoretical yield limit of the structure. Evidently, the isolated bridge performs significantly better than the non-isolated one. Deck accelerations (and accordingly forces in the substructure) are lower by factors of the order of 4 to 6.

A large number of tests were conducted with the higher friction isolation system ($f_{max} = 0{\cdot}10$ to $0{\cdot}12$). This system is appropriate for application in areas of strong seismicity because of its higher energy dissipation capability. However, the system was tested for a wide range of level of excitation. The recorded peak substructure response in these tests of the isolated bridge with flexible piers is presented in Figure 6. Input being the motions of Table II scaled to have peak accelerations in the range of 0·1 to about $1{\cdot}1g$, the pier shear force is maintained, under elastic conditions, between about 0·15 and 0·27 of the gravity axial load. This marked insensitivity of the response to the level and content in frequency of the excitation is in contrast to the response of the non-isolated bridge, which is also shown in Figure 6.

Moreover, Figure 7 shows the bearing displacement response of the isolated bridge in the same tests. It may be noted that the peak bearing displacement is, in general, of the same order as or less than the peak table (ground) displacement. Of interest is to note the recorded permanent displacements in the same tests. While the peak substructure and bearing displacement response are nearly the same in the two systems (with $f_{max} = 0{\cdot}10$ and $0{\cdot}12$), the permanent displacements differ substantially in the two systems. The system with low value of the near zero sliding velocity friction coefficient (f_{min}—see Figure 4) has substantially lower permanent displacements than the other system.

Table II. Earthquake motions used in test program and characteristics in prototype scale

Notation	Record	Peak ACC. (g)	Peak VEL. (mm/sec)	Peak dis. (mm)
El Centro	Imperial Valley, 18 May, Component S00E	0·34	334·50	108·70
Taft	Kern County, 21 July, 1952, Component N21E	0·16	157·20	67·10
Mexico	Mexico City, 19 September, 1985 SCT building, Component N90W	0·17	605·00	212·00
Pacoima S16E	San Fernando, 9 February, 1971, Component S16E	1·17	1132·30	365·30
Pacoima S74W	San Fernando, 9 February, 1971, Component S74W	1·08	568·20	108·20
Hachinohe	Tokachi, Japan, 16 May, 1968 Hachinohe, Component N-S	0·23	357·10	118·90
Miyagiken oki	Miyaki, Japan, 12 June, 1978 Ofunato-Bochi, Component E-W	0·16	141·00	50·80
Akita	Nihonkai Chuubu, Japan, 23 May, 1983 Component N-S	0·19	292·00	146·00
JP. L1G1	Artificial Compatible with Japanese Level 1 Ground Condition 1	0·10	215·00	90·00
JP. L1G2	Artificial Compatible with Japanese Level 1 Ground Condition 2	0·12	251·00	69·00
JP. L1G3	Artificial Compatible with Japanese Level 1 Ground Condition 3	0·14	274·00	132·00
JP. L2G1	Artificial Compatible with Japanese Level 2 Ground Condition 1	0·37	864·00	526·00
JP. L2G2	Artificial Compatible with Japanese Level 2 Ground Condition 2	0·43	998·00	527·00
JP. L2G3	Artificial Compatible with Japanese Level 2 Ground Condition 3	0·45	1121·00	700·00
CalTrans 0·6g A2	Artificial Compatible with CalTrans 0·6g 80′–150′ Alluvium Spectrum, No. 2	0·60	836·40	282·90
CalTrans 0·6g S2	Artificial Compatible with CalTrans 0·6g 10′–80′ Alluvium Spectrum, No. 2	0·60	765·00	248·90
CalTrans 0·6g S3	Artificial Compatible with CalTrans 0·6g 10′–80′ Alluvium Spectrum, No. 3	0·60	778·00	438·90
CalTrans 0·6g R1	Artificial Compatible with CalTrans 0·6g Rock Spectrum, No. 1	0·60	530·90	443·80
CalTrans 0·6g R2	Artificial Compatible with CalTrans 0·6g Rock Spectrum, No. 2	0·60	510·00	274·30
CalTrans 0·6g R3	Artificial Compatible with CalTrans 0·6g Rock Spectrum, No. 3	0·60	571·00	342·40

Table III. Comparison of response of isolated (case of low friction) and non-isolated bridge

Excitation	Isolated (f_{max} = 0·058)			Non-isolated	
	Deck acc. (g)	Peak bearing displ. (mm)	Perm. bearing displ. (mm)	Deck acc. (g)	Displ. of deck w.r.t.table (mm)
El Centro 25%	N.A.	N.A.	N.A.	0·25	4·9
El Centro 50%	0·08	5·6	1·7	0·50	9·8*
El Centro 100%	0·10	16·0	0·9	N.A.	
Taft 75%	N.A.	N.A.	N.A.	0·25	5·0
Taft 100%	0·08	3·5	0·5	0·33	6·6*
Taft 200%	0·09	15·3	0·5	N.A.	
Taft 300%	0·14	37·0	0·5	N.A.	
Miyagikenoki 75%	N.A.	N.A.	N.A.	0·22	4·9
Miyagikenoki 130%	0·09	5·0	0·5	0·51	11·4
Hachinohe 50%	N.A.	N.A.	N.A.	0·18	4·0
Hachinohe 100%	0·10	14·2	3·7	0·36	8·0

*Extrapolated from lower amplitude tests

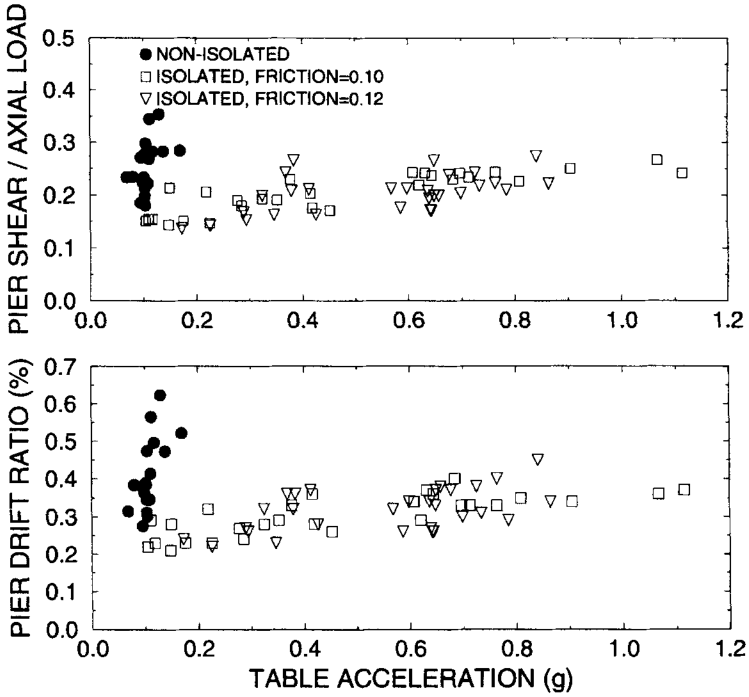

Figure 6. Comparison of substructure response of non-isolated and isolated high friction bridge system

The results of Figures 6 and 7 demonstrate the significant benefits offered by seismic isolation. As expected, the tested high friction (or, in general, high characteristic strength) isolation systems have been effective in strong seismic excitation. Interestingly, the same systems have been also effective in weak seismic excitation. A notable example of this behaviour has been the response of the f_{max} = 0·10 system in the weak level 1 Japanese bridge design motions. Figure 8 compares recorded loops of pier shear force versus pier drift of the isolated and non-isolated bridges in these Japanese motions for the three soil conditions (G.C. 1 = rock, G.C. 3 = deep alluvium). Evidently, the isolated bridge develops approximately one half the shear force and

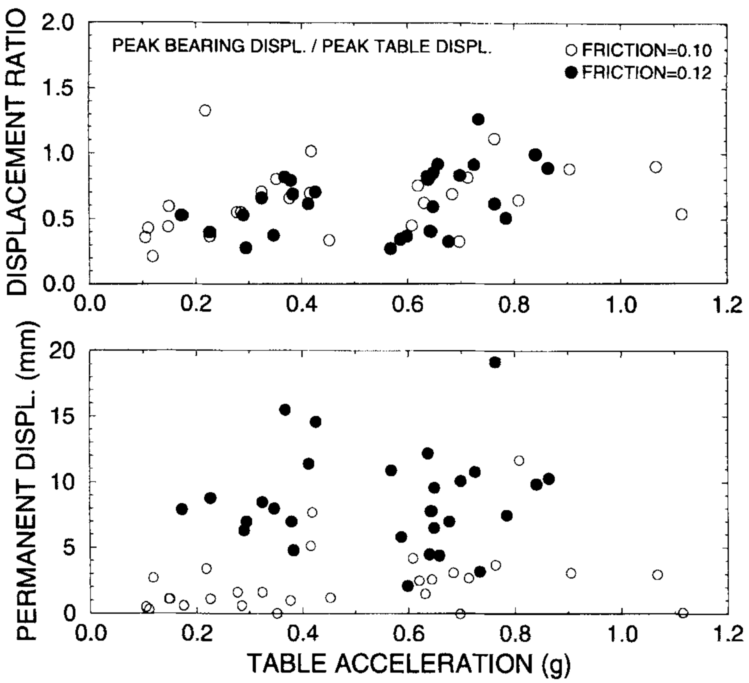

Figure 7. Recorded displacement response of isolated bridge with high friction bearings

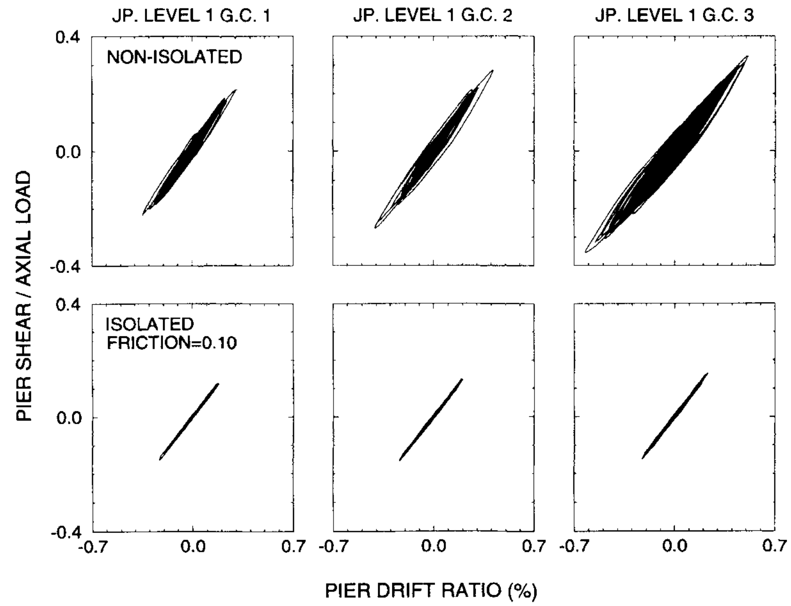

Figure 8. Comparison of substructure response of non-isolated and isolated bridges with high friction bearings in the weak Japanese level 1 bridge design motions

drift in its piers than the non-isolated bridge. Moreover, the response of the isolated bridge shows a marked insensitivity to the frequency content of the input. This desirable behaviour of the high friction system in weak excitation is the result of the velocity dependence of the friction force.

The effect of vertical ground motion has been studied in selected tests, in which the seismic motion was applied with and without the vertical component. Of these, the most notable has been a test with the Taft

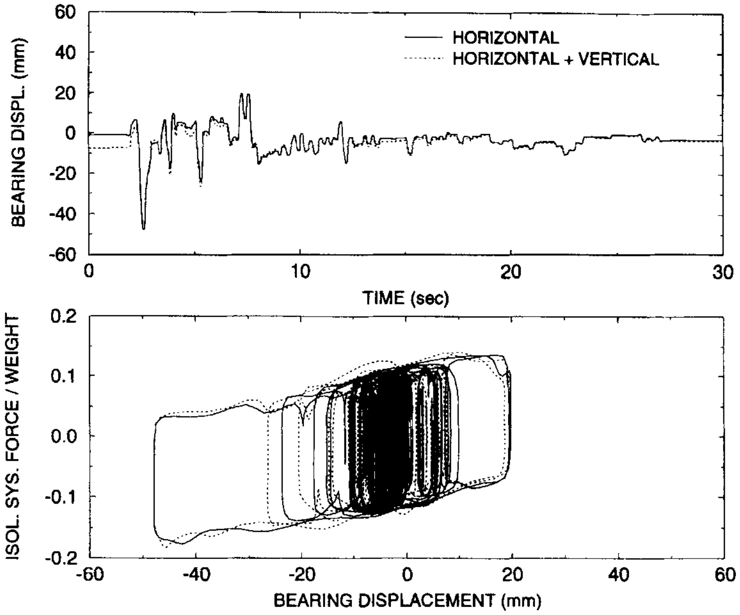

Figure 9. Comparison of response of isolated bridge (flexible pier case, material No. 1, $f_{max} = 0{\cdot}10$) for horizontal only and horizontal plus vertical Taft 400 per cent input

earthquake scaled up by a factor of four. The peak horizontal acceleration reached $0{\cdot}69g$, whereas the peak vertical acceleration reached $0{\cdot}5g$. Figure 9 compares the recorded response of the isolated bridge with friction coefficient of $f_{max} = 0{\cdot}1$ in the tests with this motion and with and without the vertical component. The effect of vertical ground acceleration is minor. This may appear as inconsistent with equation (2), in which the instantaneous axial load is

$$W^* = W\left(1 + \frac{\ddot{u}_{gv}}{g}\right) \tag{5}$$

where W is the gravity load and $\ddot{u}_{gv}$ is the vertical acceleration at the bearing level. Since the peak value of the vertical acceleration was $0{\cdot}5g$, one would expect, in the case of vertical input, variations in the isolation system force of about ± 50 per cent of the value recorded in the test without vertical input. Indeed this occurred, but at a time in which the bearing displacement was small so that the peak isolation system was only marginally affected.

ANALYTICAL PREDICTION OF RESPONSE

The tested isolation bridge model was modelled in sufficient detail to account for the effects of pier flexibility, pier top rotation, pier energy dissipation and dependency of bearing lateral force on sliding velocity and instantaneous normal force. The bearing lateral force was described by equations (2)–(5) with the parameters of Table I for the case of material No. 1. Details of the analytical model and a large number of comparisons of analytical and experimental results may be found in Constantinou *et al.*[7] Herein we present a comparison of experimental and analytical results only for one case. This is the aforementioned test with the Taft motion, scaled up by a factor of four and including the vertical component. The piers were flexible and the bearing material was No. 1 ($f_{max} = 0{\cdot}10$). The results are presented in Figure 10. The accuracy of the analytical prediction is seen to be very good.

The analytical model of the tested bridge structure was used in predicting the peak response for a range of values of the friction coefficient. Results were obtained for the motions Taft 400 per cent, horizontal and

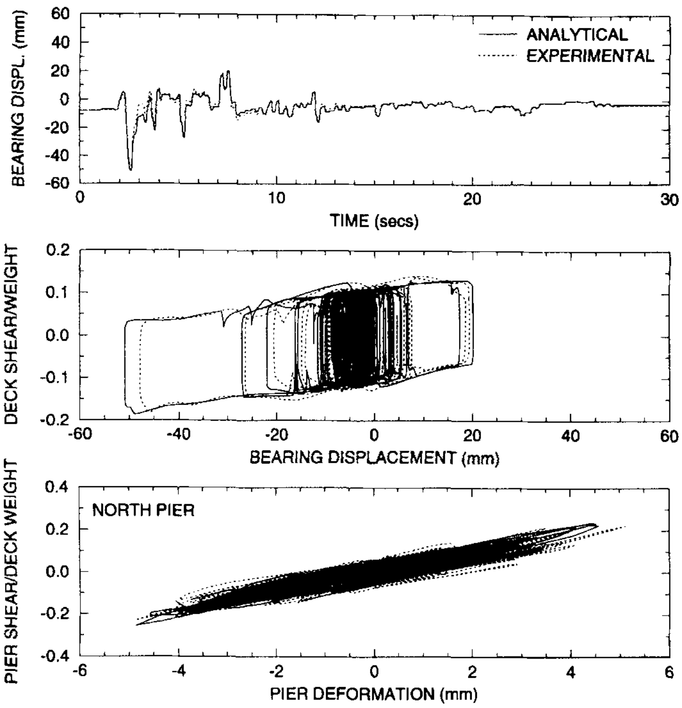

Figure 10. Comparison of experimental and analytical results in test with Taft 400 per cent H + V input

vertical (peak horizontal acceleration = 0·69g, peak vertical acceleration = 0·5g), El Centro 200 per cent, horizontal and vertical (peak horizontal acceleration = 0·65g, peak vertical acceleration = 0·35g) and the long-period Japanese level 2, ground condition 2 bridge design motion (peak horizontal acceleration = 0·42g). The coefficient of friction followed equation (4) with value f_{max}, at high velocity of sliding, in the range of 0·05 to 0·15. The value of the friction coefficient at nearly zero velocity, f_{min}, was assumed to be 0·4f_{max}. The results on the peak bearing displacement (at the quarter length scale of the tested model) and peak pier shear force are presented in Figure 11. The experimental results for the bearings with material No. 1 (see Table I—f_{max} = 0·104) are included in the figure and they are in good agreement with the analytical results.

A number of observations can be made in the results of Figure 11. An interesting one is that increases in the coefficient of friction (or characteristic strength in the general case of a non-linear system) may result in substantial reductions in bearing displacement (an expected phenomenon) or may result in only minor changes in this displacement. This latter result appears to contradict intuition. Actually, the authors[6] produced experimental results, although with another isolation system, which demonstrate this phenomenon. The system consisted of flat sliding bearings with f_{max} equal to either 0·14 or 0·07 and rubber restoring force devices, and it was tested with the same bridge model with flexible piers. The effective period of the isolation system, in the absence of friction, was 1·33 sec, thus not very different from that of the tested FPS system (1·5 sec). Figure 12 compares time histories of bearing displacements of the two systems in the Hachinohe motion, scaled up to a peak table acceleration of 0·46g (the interested reader is referred to the report of Tsopelas *et al.*,[6] tests No. RHHRUN48 and RLLRUN33, for more details). Despite the substantial differences in friction, the two systems responded with nearly identical peak bearing displacements. An explanation for this behaviour may be found in the fact that this earthquake caused the peak bearing response to occur in the first cycle, when neither system dissipated sufficient seismic energy.

Another important observation is that substantial changes in the friction coefficient result in moderate changes in the pier shear force. Most notable is the response in the Japanese motion where the pier shear

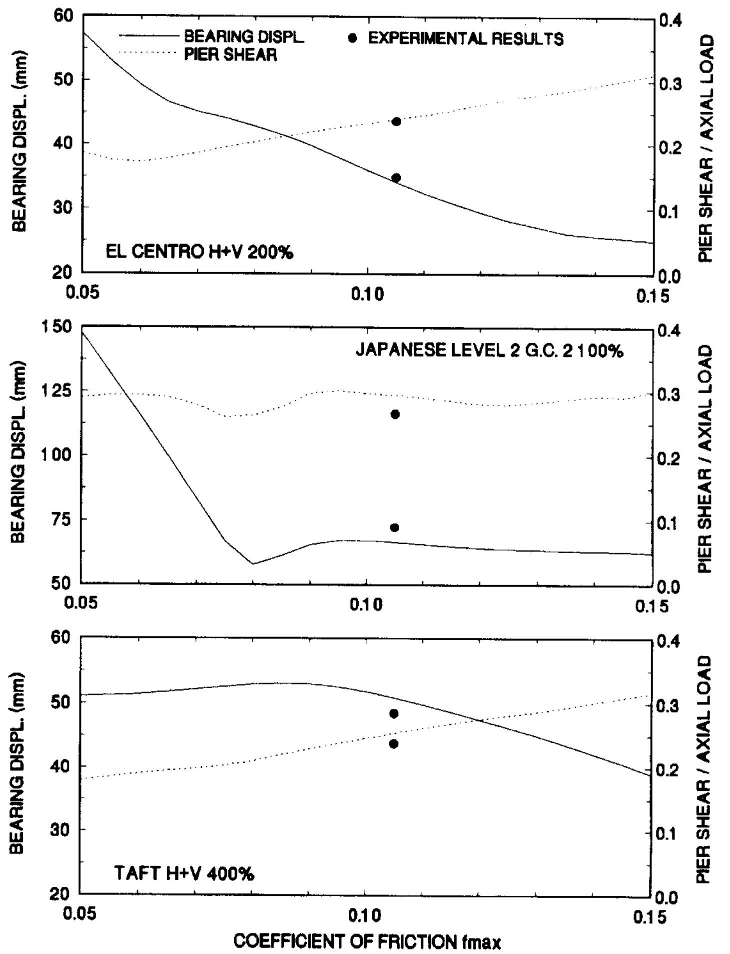

Figure 11. Analytical predicted response of bridge model with flexible piers for a range of friction values

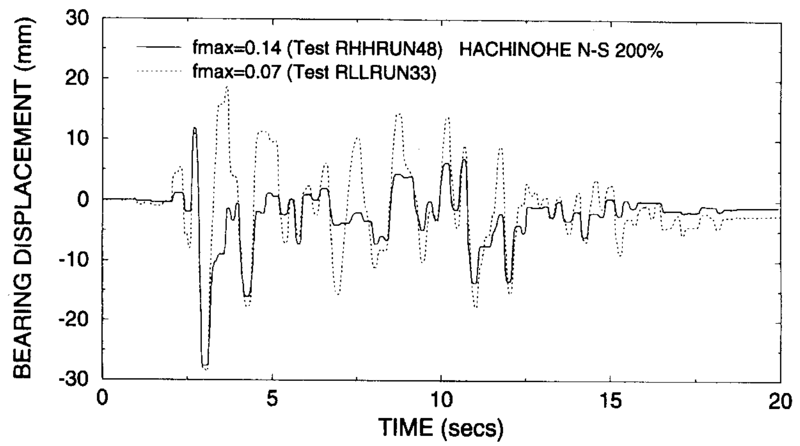

Figure 12. Comparison of time histories of bearing displacement of another isolation system with $f_{max} = 0{\cdot}14$ and 0·07, and period of 1·33 sec (same bridge model, quarter length scale)

force is practically unchanged for a three-fold increase of the coefficient of friction. More typical, however, is the behaviour in the scaled El Centro and Taft earthquakes (both are strong with peak horizontal acceleration of about $0{\cdot}7g$ and peak vertical acceleration of 50 to 70 per cent of the horizontal one). A practical design of an isolation system may have a friction coefficient $f_{max} = 0{\cdot}07$ (it will require a fairly high bearing pressure so that a compact design may be achieved). For both earthquakes, the pier shear is equal to about 20 per cent of the gravity load. An increase of the coefficient to 0·105 (a 50 per cent increase) will result in a pier shear of about 25 per cent of the gravity load, whereas an increase of the coefficient to 0·14 (a 100 per cent increase) will result in a pier shear of 30 per cent of the gravity load. Thus, substantial increases in the coefficient of friction resulted in a moderate increase in the bridge substructure forces.

CONCLUSIONS

Experimental results for an isolated bridge with FPS bearings demonstrated substantial reduction of inertia forces in comparison to a comparable non-isolated bridge. In particular, for the tested configuration with flexible piers and dynamic coefficient of friction in the range of 0·10 to 0·12, the seismic input consisted of an array of actual and simulated motions with peak horizontal acceleration in the range of 0·1 to $1{\cdot}1g$. Recorded pier shear forces ranged between 0·15 and 0·27 of the gravity axial load and peak bearing displacements were of the same order or less than the peak table (ground) displacement.

The isolated bridge even demonstrated better performance than the non-isolated one in weak seismic excitation as a result of the velocity dependence of the friction force. Moreover, tests conducted with and without the vertical component of ground motion resulted in minor differences in response.

An analytical model of the tested bridge model predicted the recorded response with good accuracy. This analytical model was then utilized to extend the experimental results over a wide range of friction values. The results showed that substantial increases in the coefficient of friction result in moderate increase in the substructure forces. However, it has been shown by analysis and confirmed by experiment that for particular types of earthquake motion it is possible to have substantial increase in friction force (or, in general, characteristic strength of non-linear isolation systems) without affecting the peak displacement response of the isolation system. This result appears to contradict intuition, in which increases in friction force result in increased dissipation of energy; thus, reduction of displacement.

ACKNOWLEDGEMENTS

This work has been supported by the National Center for Earthquake Engineering Research and Taisei Corporation, Japan. The FPS bearings were manufactured by Earthquake Protection Systems, Inc., San Francisco, CA, U.S.A.

REFERENCES

1. R. L. Mayes, 'Seismic isolation of bridges in the U.S.A.' in *Proc., 3rd U.S.–Japan workshop on earthquake protective systems for bridges*, Berkeley, California, *Report No. NCEER 94-0009,* National Center for Earthquake Engineering Research, State University of New York, Buffalo, NY, 1994.
2. T. T. Soong and M. C. Constantinou (ed.), *Passive and Active Structural Vibration Control in Civil Engineering,* Springer, Wien, 1994.
3. R. Medeot, 'The evolution of seismic devices for bridges in Italy', in *3rd world congress on joint sealing and bearing systems for concrete structures, Vol. 2,* Toronto, Canada, 1991, pp. 1295–1320.
4. P. Tsopelas and M. C. Constantinou, 'NCEER–Taisei Corporation research program on sliding seismic isolation systems for bridges—experimental and analytical study of a system consisting of lubricated PTFE sliding bearings and mild steel dampers' *Report No. NCEER 94-0022,* National Center for Earthquake Engineering Research, State University of New York, Buffalo, NY, 1994.
5. K. Kawashima and S. Unjoh, 'Menshin design of highway bridges in Japan', in *Proc. 3rd U.S.–Japan workshop on earthquake protective systems for bridges,* Berkeley, CA, *Report No. NCEER 94-0009,* National Center for Earthquake Engineering Research, State University of New York, Buffalo, NY, 1994.
6. P. Tsopelas, S. Okamoto, M. C. Constantinou, D. Ozaki and S. Fujii, 'NCEER–Taisei Corporation research program on sliding seismic isolation systems for bridges—experimental and analytical study of systems consisting of sliding bearings, rubber restoring force devices and fluid dampers', *Report No. NCEER 94-0002,* National Center for Earthquake Engineering Research, State University of New York, Buffalo, NY, 1994.
7. M. C. Constantinou, P. Tsopelas, Y.-S. Kim and S. Okamoto, 'NCEER–Taisei Corporation research program on sliding seismic isolation systems for bridges—experimental and analytical study of friction pendulum system (FPS)', *Report No. NCEER 93-0020,* National Center for Earthquake Engineering Research, State University of New York, Buffalo, NY, 1993.

8. V. A. Zayas, S. S. Low and S. A. Mahin, 'The FPS earthquake resisting system, experimental report', *Report No. EERC 87-01*, Earthquake Engineering Research Center, University of California, Berkeley, CA, 1987.
9. A. Mokha, M. C. Constantinou, A. M. Reinhorn and V. A. Zayas, 'Experimental study of friction pendulum isolation system', *J. struct. eng. ASCE* **117**, 1201–1217 (1991).
10. T. M. Al-Hussaini, V. A. Zayas and M. C. Constantinou, 'Seismic isolation of multi-story frame structures using spherical sliding isolation systems', *Report No. NCEER 94-0007*, National Center for Earthquake Engineering Research, State University of New York, Buffalo, NY, 1994.
11. Civil Engineering Research Center-CERC, 'Manual of Menshin design method for highway bridges', Ministry of Construction, Japan, 1992 (in Japanese).
12. J. H. Gates, 'Factors considered in the development of the California seismic design criteria for bridges', in *Proc. workshop on earthquake resistance of highway bridges*, Applied Technology Council, Palo Alto, CA, 1979, pp. 141–162.
13. M.C. Constantinou, A. Kartoum, A. M. Reinhorn and P. Bradford, 'Experimental and theoretical study of a sliding isolation system for bridges', *Report No. NCEER 91-0027*, National Center for Earthquake Engineering Research, State University of New York, Buffalo, NY, 1991.